Biology of Reproduction, 2021, 104(2), 325–335
doi:10.1093/biolre/ioaa215
Research Article
Advance Access Publication Date: 27 November 2020

OXFORD

Research Article

ZC3H4—a novel Cys-Cys-Cys-His-type zinc finger protein—is essential for early embryogenesis in mice†

Jianmin Su[1,2,‡], Xiaosu Miao[1,‡], Danielle Archambault[1], Jesse Mager[1,*] and Wei Cui[1,3,*]

[1]Department of Veterinary and Animal Sciences, University of Massachusetts, Amherst, MA, USA, [2]Key Laboratory of Animal Biotechnology of the Ministry of Agriculture, College of Veterinary Medicine, Northwest A&F University, Yangling, Shaanxi, PR China and [3]Animal Models Core Facility, Institute for Applied Life Sciences (IALS), University of Massachusetts, Amherst, MA, USA

*__Correspondence:__ Department of Veterinary and Animal Sciences, University of Massachusetts, Amherst, MA 01002, USA. E-mail: jmager@vasci.umass.edu (J. Mager), wcui@umass.edu (W. Cui)

†__Grant Support:__ This work was supported by faculty start-up funds (WC) and by NIH grant R01HD083311 (JM).
‡Jianmin Su and Xiaosu Miao have contributed equally to this work.

Received 28 June 2020; Revised 10 October 2020; Accepted 25 November 2020

Abstract

Zinc finger domains of the Cys-Cys-Cys-His (CCCH) class are evolutionarily conserved proteins that bind nucleic acids and are involved in various biological processes. Nearly 60 CCCH-type zinc finger proteins have been identified in humans and mice, most have not been functionally characterized. Here, we provide the first in vivo functional characterization of ZC3H4—a novel CCCH-type zinc finger protein. Our results show that although *Zc3h4* mutant embryos exhibit normal morphology at E3.5 blastocyst stage, they cannot be recovered at E7.5 early post-gastrulation stage, suggesting implantation failure. Outgrowth assays reveal that mutant blastocysts either fail to hatch from the zona pellucida, or can hatch but do not form a typical inner cell mass colony, the source of embryonic stem cells (ESCs). Although there is no change in levels of reactive oxygen species, *Zc3h4* mutantsdisplay severe DNA breaks and reduced cell proliferation. Analysis of lineage specification reveals that both epiblast and primitive endoderm lineages are compromised with severe reductions in cell number and/or specification in the mutant blastocysts. In summary, these findings demonstrate the essential role of ZC3H4 during early mammalian embryogenesis.

Summary sentence

ZC3H4 is essential during early embryo development in vivo, loss of ZC3H4 results in defective epiblast and primitive endoderm lineages, severe DNA breaks, reduced cell proliferation, and failure to develop beyond blastocyst formation.

Key words: Blastocyst embryo, inner cell mass, cell lineage specification, epiblast, DNA break.

Introduction

Preimplantation development in mammals involves four stages: oocyte fertilization, embryo cleavage, morula, and blastocyst formation [1, 2]. To form a competent blastocyst stage embryo that is capable of uterine implantation, the newly formed zygote undergoes a series of cleavage divisions resulting in increasing numbers of smaller blastomeres [3, 4]. During this period, three major transcriptional and morphogenetic events also take place concurrently. The first event, maternal-to-zygotic transition, initiates the degradation of maternal mRNAs and proteins with replacement from zygotic transcripts [5, 6]. Upon reaching 8-cell stage in the mouse, embryo initiates the second major event, compaction, and polarization [3, 4]. Following this, the third critical event occurs, which is blastomere cell fate allocation resulting in the outer polar cells differentiating exclusively into the trophectoderm (TE), whereas the apolar cells located inside of the morula give rise to the inner cell mass (ICM) [7, 8]. When the blastocyst contains 32–64 cells, the ICM separates into the pluripotent epiblast (EPI) lineage and the primitive endoderm (PE) lineage [9]. These first three lineages (EPI, PE, and TE) will give rise to the embryo, parietal yolk sac, and placenta, respectively [10, 11].

Lineage specification during early mammalian embryogenesis is a highly regulated process that relies on the differential expression of various genes within distinct cell populations [12, 13]. Specific localization of transcription factors (TFs) and differential gene expression profiles have been illustrated in blastocyst embryos of different mammalian species [14–16]. For example, to establish and maintain the cell fate in mouse embryos, the TF CDX2 is enriched in TE, whereas OCT4 (alias POU5F1) becomes highly expressed in the ICM [17]. Similarly, the segregation of the EPI and PE lineages within the ICM is demarcated by Nanog homeobox (NANOG) expression in the EPI cells and SOX17 in the PE [18]. Through advances in genome manipulation, single-cell transcriptomics and loss-of-function studies, increasing numbers of genes have been found to be required during early lineage specification in mammalian embryos. For example, members of Hippo signaling pathway [18–20], Notch signaling [21], WNT signaling [22], and ROCK signaling [23, 24]. Furthermore, epigenetic regulation [25–28] and newly discovered factors, such as NOP2 [29, 30], SBNO1 [31], TFAP2C [32], SMCHD1 [6, 33], and RBBP4 [34, 35], also contribute to and dictate these unique cellular identities.

During mammalian development, zinc-finger-containing proteins represent the most abundant protein superfamily and are well known as transcriptional regulators. Among them, there is a less common family that contains tandem zinc-binding motifs characterized by three cysteines followed by one histidine (CCCH) [36, 37]. Nearly 60 CCCH-type zinc finger proteins have been identified in humans and mice; however, few have been carefully investigated in vivo. For example, *Zfp36*, *Rc3h1*, and *Zc3h12a* are critical for regulation of mRNA stability in immune cells, and each individual knockout (KO) shows similar phenotype of systemic inflammatory responses and autoimmune disease in mice [38]. Whereas *Zfp36* function is important for the immune system, *Zfp36l2* shows essential role in female fertility. Oocytes from *Zfp36l2* KO mice can be fertilized normally, however, the resultant embryos cannot progress beyond the two-cell stage [36]. Through loss-of-function experiments, ZC3H14 has been found to be a key regulator of RNA poly (A) tail length and essential for regulation of neuronal transcripts in mouse brain [39, 40] that corroborates a previous study of the orthologous *Drosophila* gene *dNab2* in neuronal development [41]. In zebrafish, the TF Zc3h8 has been shown to be required for development of multiple organs, including liver, gut, and pancreas [42]. ZC3H4, the focus of this study, has not been extensively studied at the preclinical or clinical levels, nor it been studied in embryogenesis or developmental events of any organism [43]. Up to now, it has only been examined in anaplastic thyroid carcinoma [44] and mouse lung epithelial cells [43]. Data from these cultured cells strongly suggest that ZC3H4 is essential for cell proliferation and the epithelial to mesenchymal transition, respectively.

In the present study, we use a novel knockout allele to explore the role of ZC3H4 during murine development in vivo. Our data show that ZC3H4 is essential during early embryo development in vivo, where loss of ZC3H4 results in defective EPI and PE lineages, many DNA breaks, reduced cell proliferation, and failure to implant in the uterus.

Material and methods

All chemicals and media were purchased from Millipore-Sigma (Burlington, MA, USA) unless otherwise indicated.

Generation of *Zc3h4* mutants

All procedures and methods were carried out in accordance with the approved guidelines and regulations. All animal experimental protocols were approved by the Institutional Animal Care and Use Committee of the University of Massachusetts, Amherst (2017-0071). *Zc3h4* KO allele (C57BL/6NCrl-*Zc3h4*$^{em1(IMPC)Mbp}$/Mmucd) was generated on C57BL/6NCrl background as part of the Knockout Mouse Project (KOMP) and available from the Mutant Mouse Resource & Research Centers (MMRRC, Stock #: 043477-UCD, Strain Origin: University of California, Davis). The entirety of exon 4 (ENSMUSE00000895527, 223 bp) was deleted from the *Zc3h4* gene (ENSMUST00000098789.4) to generate frame-shifted KO allele by using CRISPR/Cas9 gene editing technology in mouse zygotes (Figure 1A). Produced founders were backcrossed to C57BL/6N to produce sequence confirmed heterozygous *Zc3h4*−/*Zc3h4*+ (hereafter referred to as Het) mice (N1), which were then backcrossed again to generate Het mice (N2), in MMRRC. To expand the colony in our animal facility for the present study, Het mice from MMRRC (N2) were first backcrossed with C57BL/6N wildtype *Zc3h4*+/*Zc3h4*+ (hereafter referred to as WT) mice, and subsequent Het mice were intercrossed to generate *Zc3h4*−/*Zc3h4*− mutants (hereafter referred to as Mut). Genotyping primers used: common Forward for both WT allele and Mut allele: 5′- ACCCCACTTTCCCTCCAAAGG; Reverse for WT allele: 5′- GGCTAGGGGACAGCAGTACATGG; Reverse for Mut allele: 5′- CTTCCCTCATCTTGCCTTATGCC.

Embryo recovery, outgrowth culture, and genotyping

Zc3h4 heterozygous females (8–12 weeks old) were caged overnight with *Zc3h4* heterozygous males and examined for the presence of copulatory plugs each morning. The presence of a plug was defined as embryonic day 0.5 (E0.5). E7.5 and E3.5 embryos were collected from heterozygous females by dissection or flushing the uterus, respectively. For E7.5 embryos, embryos were imaged immediately after dissection, then collected into individual tubes for lysis and Polymerase Chain Reaction (PCR) genotyping. For E3.5 blastocysts, embryos were imaged individually in droplets and then cultured for 3 days in DMEM (Lonza, Allendale, NJ, USA) supplemented with 10% fetal bovine serum (FBS, Atlanta Biologicals, Flowery Branch, GA, USA) and 1X GlutaMAX (Thermo Fisher Scientific, Waltham,

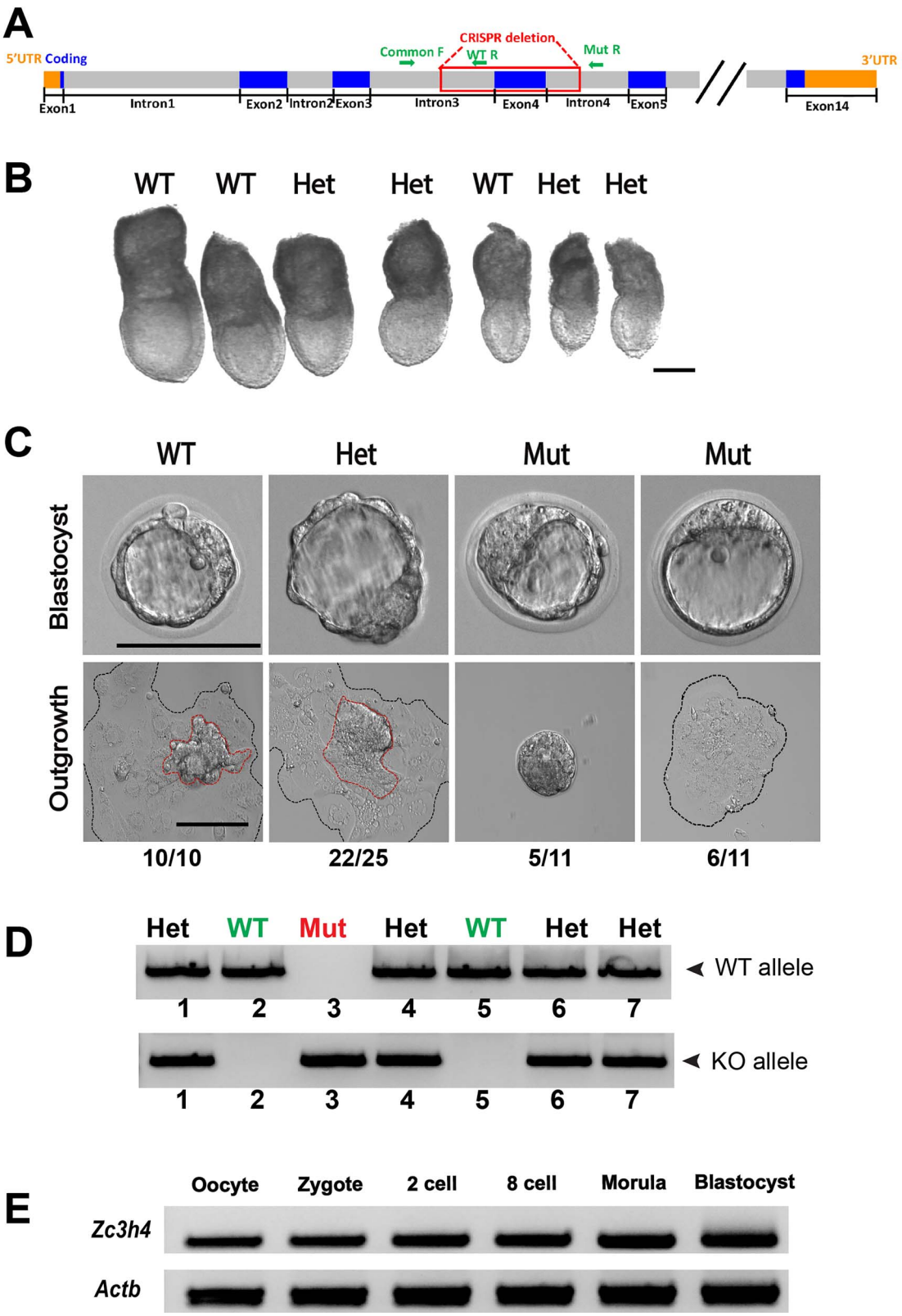

Figure 1. *Zc3h4* knock-out allele generation, embryo collection and genotyping, and expression analysis. (A) Schematic of *Zc3h4* knock-out allele generation and genotyping primers for WT allele and Mut allele. F, forward; R, reverse. (B) Representative genotyped embryos at E7.5. (C) E3.5 blastocysts from heterozygous intercrosses were imaged and subjected to 3-day-outgrowth assay before knowing the genotypes. After outgrowth culture, outgrowths were imaged again and then lysed for genotyping. Although mutant blastocysts were indistinguishable from littermates at E3.5, they do not form successful outgrowths. Outgrowths from WT and Het blastocysts displayed a distinctive ICM colony (red dashed line) surrounded by trophoblast cells (black dashed line). Mutant exhibited 2 distinct phenotypes, either failing to hatch from the zona pellucida with all blastomeres trapped in the zona (5 from 11) or they hatched but resulted in an outgrowth completely devoid of typical ICM colony (6 from 11). Scale bars, 100 µm. (D) Representative genotyping PCR of individual outgrowth. (E) RT-PCR to identify Z*c3h4* expression in WT preimplantation embryos. *Actb* was used as loading control.

MA, USA). After 3 days of culture, outgrowths were individually imaged again before lysis and genotyping. Outgrowth analysis was performed as described previously [45, 46]. Briefly, an outgrowth that displayed a distinctive ICM colony surrounded by trophoblast monolayer is considered a normal successful outgrowth, whereas outgrowths that fail to hatch, lack ICM colony or lack trophoblast monolayer are considered as failed outgrowths.

Blastocyst immunofluorescence

Immunofluorescence staining (IF) was carried out in accordance with the methods of our previous studies [46, 47]. Prior to fixation and IF, E3.5 blastocysts were harvested and cultured overnight in KSOM at 37 °C in a humidified atmosphere of 5% CO_2, 5% O_2 balanced in N_2, to further deplete the maternally-loaded protein/mRNA and also to ensure embryos had undergone EPI/PE/TE specification. After fixation in 4% paraformaldehyde and brief wash in PBS, embryos were permeabilized with 0.5% Triton X-100 in PBS containing 10% FBS for 20 min. Embryos were then blocked in blocking solution (PBS with 10% FBS and 0.1% Triton) for 1 h at room temperature, and then incubated with primary antibodies overnight at 4 °C. All primary antibodies were diluted 1:200 using the blocking solution, including: goat anti-OCT4 (abcam, ab27985); mouse anti-CDX2 (BioGenex, MU392A-UC); rabbit anti-NANOG (abcam, ab80892); rabbit anti-TRP53 (Cell Signaling Technology, #9284); goat anti-SOX17 (R&D Systems, AF1924). After three washes, embryos were incubated with suitable secondary antibodies (Alexa Fluor, Thermo Fisher Scientific, Waltham, MA, USA) for 1 h at room temperature in dark. After two washes, DNA was stained with 4,6-diamidino-2-phenylindole (DAPI) before transferring embryos into single wells of chambered slides (Corning Co., Corning, NY, USA) for imaging under a Nikon A1 Spectral Detector Confocal with FLIM Module. Z-stacks (20X objective, 8-µm sections) were collected and maximum projection applied. Embryos were handled individually such that each one was imaged and then recovered for PCR genotyping. The intensity of reactive oxygen species (ROS; green fluorescence) was analyzed using Image J software with DAPI intensity as the reference. High-resolution z-stack images were acquired under identical capture settings and intensities were measured on the raw images as described previously [48].

EdU and TUNEL labeling

Click-iT Plus EdU Cell Proliferation Kit (C10638, Thermo Fisher Scientific) was used for EdU (5-ethynyl-2′-deoxyuridine) labeling. According to the manufacturer's instructions, embryos were incubated in KSOM medium supplemented with 10-µM EdU for 25 min. Then embryos were fixed and permeabilized as mentioned in IF staining, followed by cocktail reaction of the kit to show the signal. TUNEL (terminal deoxynucleotidyl transferase dUTP nick end labeling) staining was carried out using the In Situ Cell Death Detection Kit (11684795910, Roche) according to the manual. After EdU staining, embryos were washed three times and labeled with TUNEL reaction mixture in the dark at 37 °C for 30 min. Then DNA was stained with DAPI for 10 min before embryos were individually transferred into single wells of chambered slides for imaging under confocal as described in the IF method section.

Detection of ROS

CellROX Green Reagent (C10444, Thermo Fisher Scientific) was used to detect ROS level according to the product manual. Embryos were incubated in KSOM supplemented with 5-µM CellROX Green Reagent at 37 °C for 30 min. After this, embryos were washed three times with PBS and then fixed in 4% paraformaldehyde for 20 min. Fixed embryos were then washed and individually transferred into single wells of chambered slides for imaging as described in the IF method section.

RNA extraction and reverse transcription PCR

Total RNA extraction was carried out with a Roche High Pure RNA Isolation Kit (#11828665001). Complementary DNA was synthesized using iScript cDNA synthesis kit (#170-8891; Bio-Rad Laboratories, Hercules, CA, USA). Intron-spanning primers used for reverse transcription PCR (RT-PCR): (*Actb*: 5′-GGCCCAGAGCAAGAGAG GTATCC and 5′-ACGCACGATTTCCCTCTCAGC; *Zc3h4*: 5′-GCGATGACTTCTCGGACTTC and 5′- CCTCGAGATCCTC-CTCGACT).

Embedding, sectioning, and immunofluorescence

Freshly dissected E5.5 decidua from heterozygous intercross were fixed in 4% paraformaldehyde overnight, dehydrated in ethanol, cleared in xylene, embedded with paraffin, and sectioned at 7-µm thick. The sectioned embryos were deparaffinized and rehydrated for subsequent procedures. Antigen retrieval was performed by boiling the slides in Tris-ethylenediaminetetraacetic acid (EDTA) buffer (pH 9) for 4 min and cooling to room temperature. The slides were then rinsed twice in phosphate buffered saline/0.01% Tween 20 (PBT) for 2 min and blocked with 0.5% milk in PBT for 2 h at room temperature in a humid chamber. Primary antibodies including OCT4 (Abcam, ab27985, 1: 200), CDX2 (Biogenex, AM392-5 M, 1:200), and Laminin (Sigma Aldrich, L9393, 1:250) were applied in 0.05% milk/PBT at 4 °C overnight in a humid chamber. The slides were then rinsed three times with PBT for 15 min, followed by incubation with suitable secondary antibodies at room temperature for 1 h in a humid chamber. Next, the slides were rinsed with PBS for 15 min, three times. Nuclei were counterstained with DAPI in PBS (1:10 000) for 3 min. Slides were rinsed with 1X PBS and sealed with ProLong Gold (Thermo Fisher Scientific, P36934). Fluorescent slides were imaged with Nikon Eclipse Ti inverted microscope.

Statistical analysis

All experiments were repeated at least three times and data are presented as mean ± standard error of the mean. Chi-square test was applied to the incidence of successful outgrowths, and percentage data were analyzed by analysis of variance, and differences were considered statistically significant at $P < 0.05$.

Results

Zc3h4 mutants cannot be recovered in vivo at E7.5

The *Zc3h4* knock-out allele (Stock#:043477-UCD) was generated by using CRISPR/Cas9 gene editing technology to delete the entirety of exon 4 (ENSMUSE00000895527, 223 bp) generating a frame-shifted KO allele (Figure 1A). According to the initial phenotyping analysis performed for the International Mouse Phenotyping Consortium (IMPC) [49], no homozygous *Zc3h4* mutants were born, nor found at E15.5 or E12.5 (http://www.mousephenotype.org). Therefore, we first dissected embryos at E7.5. Twenty-four embryos were recovered from four heterozygous intercrosses. Genotyping revealed 15 Het and 9 WT embryos (Figure 1B). No *Zc3h4* homozygous mutant embryos were present at E7.5, however, there was an obviously increased number of empty decidua (n = 13),

suggesting that *Zc3h4* mutants may trigger decidual response but do not produce viable gastrulation stage embryos. To gain more insight into the mechanism underlying the embryonic lethality in vivo, we collected E3.5 blastocysts for morphological assessment and 3-day-outgrowth assays. Six heterozygous intercross litters produced 46 blastocysts comprised of 11 *Zc3h4* mutants, 25 Het and 10 WT embryos. Mutant blastocysts at E3.5 were indistinguishable from littermates based on morphology alone (Figure 1C). However, 3 days of in vitro outgrowth revealed fully penetrant phenotype. Hatching and successful outgrowth rates were significantly high (Chi-square test: $P < 0.05$) for WT (100%, 10/10) and Het blastocysts (88%, 22/25), whereas none of the 11 mutants (0%, 0/11) formed a successful outgrowth (Figure 1C and D). WT and Het outgrowths displayed robust ICM colonies surrounded by trophoblast cells that were easily identified by their flattened morphology. Among 11 mutants, 5 showed failed hatching with all blastomeres still trapped in the zona and 6 exhibited no typical ICM colony (Figure 1C). These results which show defective hatching and outgrowth are consistent with a complete absence of mutant embryos at E7.5 in vivo. Based on the phenotype and timing of lethality, we evaluated *Zc3h4* expression during preimplantation stages. Due to the lack of available antibodies suitable for immunofluorescence, we performed RT-PCR and revealed that *Zc3h4* mRNA is present at all stages examined (Figure 1E).

Zc3h4 mutants have fewer ICM cells

To investigate the mechanisms underlying embryonic lethality in vivo and outgrowth failure in vitro, we first analyzed markers of apoptosis (Ser15-phospho active TRP53) and ICM/TE lineage specification on 27 blastocysts (6 WT, 17 Het, and 4 Mut) from heterozygous intercrosses (Figure 2A). Regardless of genotype, none of the embryos showed active TRP53 positive cells (Figure 2A) (positive control is shown in Supplementary Figure S1). However, cell counting revealed that *Zc3h4* mutants have significantly fewer blastomeres than Het and WT embryos (Figure 2B). Importantly, the number of both OCT4 positive cells per blastocyst (Figure 2C) and percentage of OCT4 positive cells (Figure 2D) is severely reduced in *Zc3h4* mutant blastocysts. Concordant with the decreased total cell number, the number of CDX2 positive cells per blastocyst was lower in mutants as well (Figure 2E), but the percentage of CDX2 positive cells increased significantly (Figure 2F). These results indicate that the ratio of cell allocation to each lineage is greatly altered with far fewer ICM specified cells (and more TE specified cells) in *Zc3h4* mutant embryos.

Both PE and EPI are defective in *Zc3h4* mutants

To further elucidate the mechanism and phenotype in *Zc3h4* mutant embryos, we examined the fidelity of the second lineage specification decision where ICM segregates into PE and EPI. Blastocysts recovered from heterozygous intercrosses were analyzed for the PE marker SOX17 and the EPI marker NANOG (Figure 3A). Analysis of 26 embryos (5 WT, 14 Het, and 7 Mut) revealed a significantly reduced number and percentage of both NANOG-positive EPI cells (Figure 3C and D) and SOX17-positive PE cells (Figure 3E and F), when compared with WT and Het littermates. Concordant with decreased PE and EPI ratios, a significant increase in the percent of CDX2-positive TE cells was detected (Figure 3G). These results suggest that both PE lineage and EPI lineage are defective with far fewer cells in the absence of ZC3H4.

Zc3h4 mutants display many DNA breaks and reduced proliferation

Since *Zc3h4* mutants have reduced total cell numbers, we next performed fluorescent whole-mount TUNEL assays and EdU labeling to assay DNA breaks and cell proliferation, respectively (Figure. 4A), on 25 blastocysts (6 WT, 12 Het, and 7 Mut). These assays showed that Mut embryos exhibited a significantly higher percentage of TUNEL-positive nuclei (Figure 4B), indicating that loss of ZC3H4 results in increased DNA breaks and cell death. EdU labeling demonstrated a markedly decreased percentage of EdU-positive cells in these *Zc3h4* mutants (Figure 4C), indicating that many fewer cells are proliferating in the absence of ZC3H4.

We next assessed the levels of reactive oxygen species (ROS), which has been used as marker for oxidative homeostasis and general cell viability/health [48, 50]. Our result showed that all genotypes exhibited similarly low levels of ROS, suggesting that ZC3H4 does not significantly regulate or alter oxidative homeostasis during early mammalian embryogenesis (Figure 5) (positive control is shown in Supplementary Figure S2).

Discussion

Early embryogenesis is a highly regulated process that relies on the differential expression of various genes at specific stages and in distinct cell populations. With the advent of large-scale transcriptome profiling, more than 11 000 genes have been detected during mammalian preimplantation development. Zinc finger proteins (ZFPs) are one of the most abundant groups of genes expressed during this developmental window [36, 51]. Compared with other types of ZFPs (such as C2H2-type and RING-type), CCCH-type is much less common and most CCCH-type ZFPs have not been characterized during various cellular events and biological processes [40, 52]. In the present study, we use a novel knockout allele and for the first time demonstrate the essential role of ZC3H4 during murine development in vivo. Although *Zc3h4* mutants look normal at E3.5, these blastocysts cannot successfully outgrow in vitro that is consistent with the absence of E7.5 mutants in vivo. To the best of our knowledge, this is the first CCCH-type ZFP that causes peri-implantation lethality when knocked out. Notably, the apparent increase in empty decidua at E7.5 (n = 13 from 4 intercross litters, along with 15 Hets and 9 WTs) suggests that most *Zc3h4*-KO embryos elicit a decidual response, but likely degenerate and resorb such that no embryo can be isolated at later stages, a phenotype that has been documented for other KO alleles [53–55]. Our lineage analysis suggests significant defects in ICM/EPI/PE but not in TE specification. However, implantation failure certainly indicates defective TE function. Signaling from the ICM has been well documented to be required for TE function at peri-implantation stages [56]. Therefore, one obvious possibility is that TE in *Zc3h4* mutants does not receive appropriate signals from the mutant ICM to fully differentiate and facilitate successful implantation and further development. In order to assess mutant embryo implantation in vivo, we performed immunofluorescence analysis on E5.5 decidua from heterozygous intercross. Among 9 deciduae, 6 contained normal E5.5 embryo structures with radially symmetric egg-cylinder morphology and appropriate OCT4 and CDX2 expression. However, the other 3 decidua had tiny round structures in the midst of normal sized maternal decidual cells which were neither OCT4 nor CDX2 positive (Supplementary Figure S3). Since the occurrence fits mendelian frequency (3/9) and we observe similar percentage of empty decidua at E7.5, we assume these are

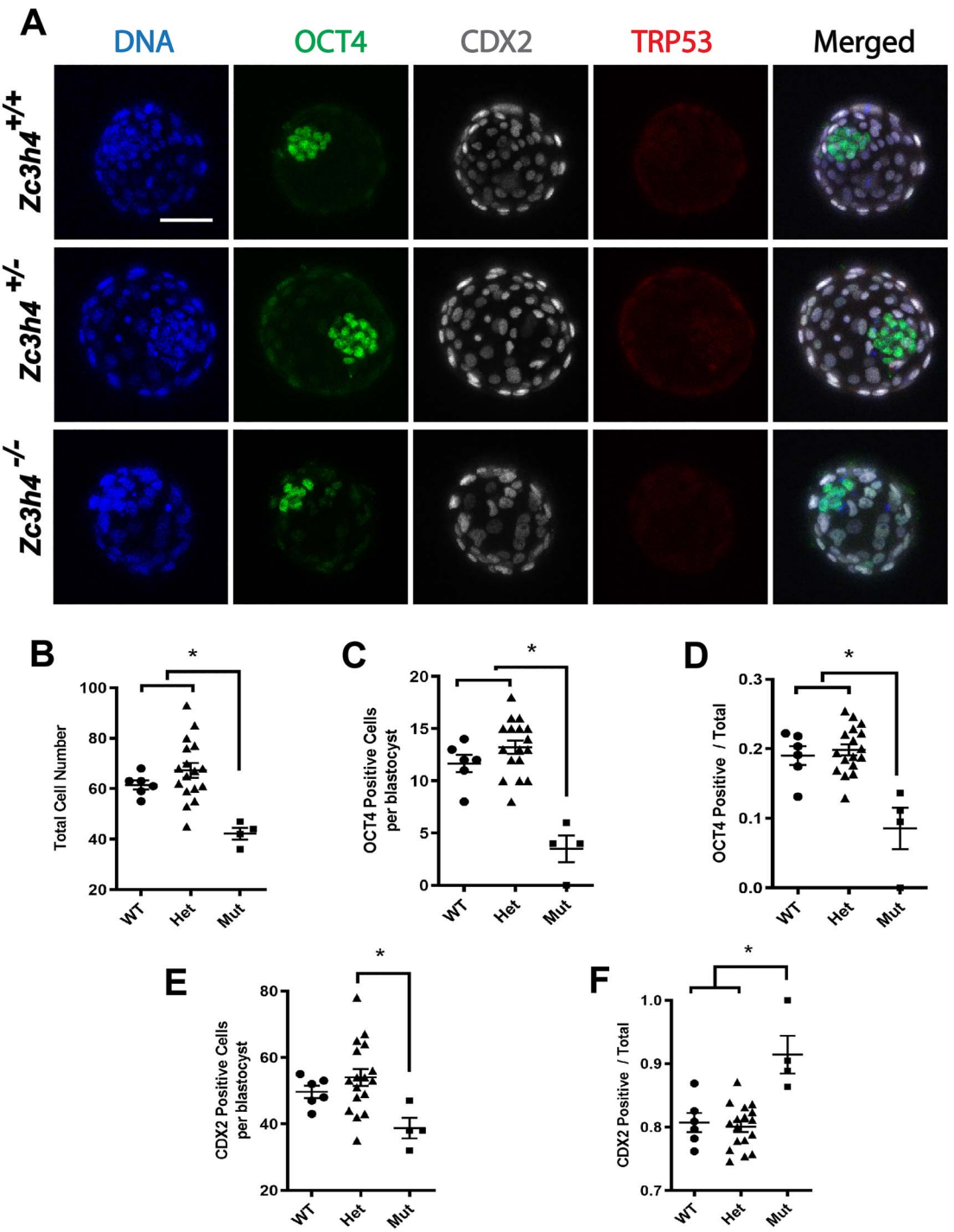

Figure 2. Decreased total cell number and altered lineage allocation was found in *Zc3h4* mutant embryos. (A) IF of OCT4 (ICM marker), CDX2 (TE marker), and active TRP53 (apoptosis marker) in blastocysts of different genotypes. (B) Total cell number per blastocyst in Mut embryos was significantly decreased. (C) The number of OCT4 positive cells per blastocyst was severely reduced in Mut embryos. (D) The percentage of ICM cells (OCT4 positive) in Mut embryos was significantly decreased. (E) The number of CDX2 positive cells per blastocyst was severely reduced in *Zc3h4* mutants. (F) The percentage of CDX2-positive TE cells was significantly increased in *Zc3h4* mutants. Scale bar, 50 μm. *, $P < 0.05$.

remnants of the *Zc3h4* mutant embryos (we cannot genotype cleanly after sectioning within decidua). These results suggest that mutant embryos do contact the maternal uterine epithelium and induce a similar decidualization, but do not develop further than blastocyst stage. Further experiments are needed to determine if ZC3H4 is required only in the ICM or in all early lineages at different stages.

OCT4, encoded by gene *Pou5f1*, is a homeodomain TF of POU family and has been shown to be a key regulator during early

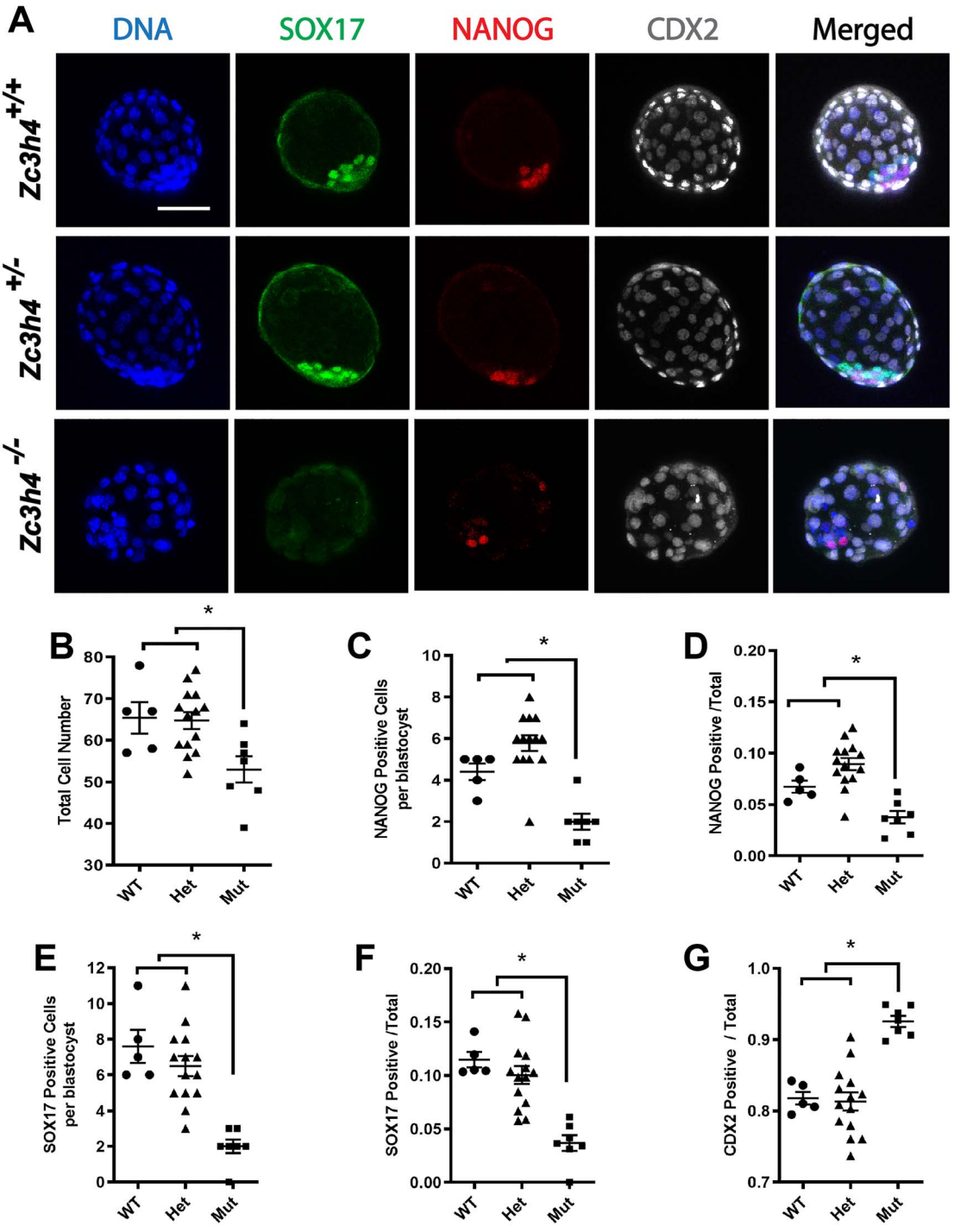

Figure 3. Both PE and EPI are defective in *Zc3h4* mutant embryos. (A) IF of SOX17 (PE marker), NANOG (EPI marker), and CDX2 (TE marker) in blastocysts of different genotypes. (B) The total cell number per blastocyst in *Zc3h4* mutant embryos is decreased, as well as a significantly reduced number (C) and percentage (D) of NANOG-positive EPI cells when compared with WT and Het littermates. A significantly reduced number (E) and percentage (F) was found for SOX17-positive PE cells when compared with WT and Het littermates. (G) Concordant with decreased PE and EPI ratios, a significant increase in the percent of CDX2-positive TE cells was detected in *Zc3h4* mutants. Scale bar, 50 μm. *, $P < 0.05$.

embryonic development and ICM lineage specification [57, 58]. Our study demonstrates a 50% reduction in the number of OCT4-positive cells in the absence of ZC3H4, with concomitant reduction in both NANOG-positive EPI cells and SOX17-positive PE cells. These results are consistent with previous findings that NANOG expression is directly regulated by OCT4 [59, 60] and that sustained OCT4 expression is required for PE specification [61]. Importantly, defective ICM has also been reported with loss-of-function in other

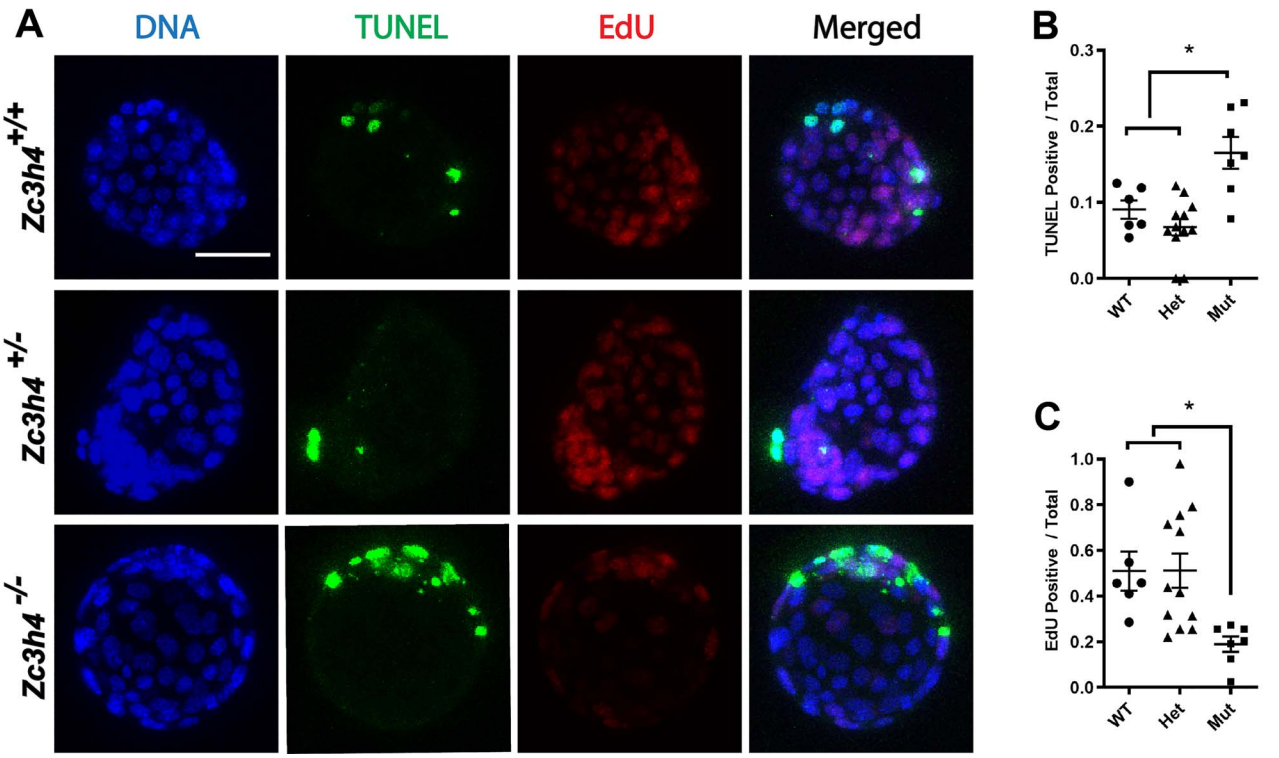

Figure 4. Increased DNA breaks and decreased cell proliferation were found in *Zc3h4* mutant embryos. (A) Fluorescent whole-mount TUNEL assay and EdU labeling assay were performed to see if ZC3H4 is involved in DNA breaks and cell proliferation, respectively. (B) *Zc3h4* Mut blastocysts exhibited a significantly higher percentage of TUNEL-positive nuclei when compared with WT and Het littermates. (C) Percentage of EdU-positive nuclei was markedly decreased in *Zc3h4* mutant blastocysts when compared with WT and Het littermates. Scale bar, 50 μm. *, $P < 0.05$.

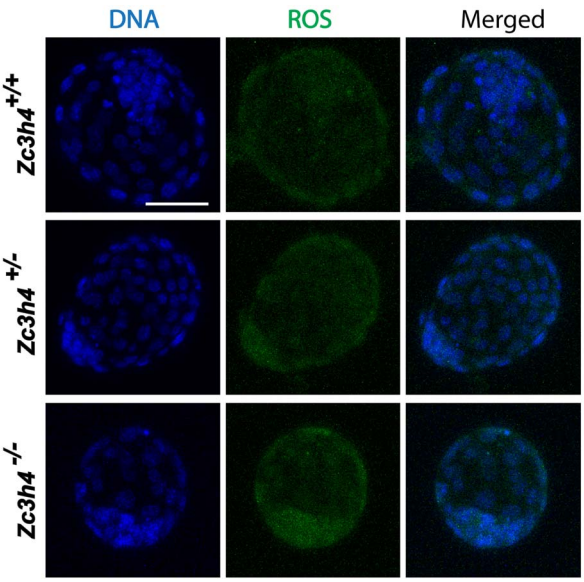

Figure 5. IF of ROS (marker for oxidative homeostasis and general cell viability/health) in blastocysts of different genotypes. All genotypes displayed similarly low ROS levels, suggesting that ZC3H4 does not significantly regulate or alter oxidative homeostasis during early embryo development in mice. Scale bar, 50 μm.

genes, such as *Gins1* [62], *Setd1a* [63], *Med28* [64], and *Rbbp4* [35], suggesting that different genes may participate in a common pathway or mechanism involved in ICM development and function.

It is noteworthy that, ICM formation and morphology look normal in absence of OCT4 [65]. However, in this study, KO of *Zc3h4* reduced the number of cells contributing to the ICM (Figure 2D), suggesting that *Zc3h4* may act upstream of *Oct4* expression during early development of embryonic pluripotency. In fact, ZC3H13, another CCCH-type ZFP, was recently discovered as a key factor that promotes mouse embryonic stem cell (ESC) self-renewal and pluripotency through facilitating m^6A methylation [66]. Given the known fact that some CCCH-type ZFPs (e.g., ZFP36, RC3H1, and ZC3H12A) can regulate the steady-state and translation of their target RNAs [38], another possibility is that ZC3H4 may also facilitate post-transcriptional regulation of target mRNAs that are essential for cell lineage specification.

It has been previously shown that a minimum of 4 NANOG-positive EPI cells are needed at the blastocyst stage for normal embryo development to proceed [67]. Consistent with this report, our data show that majority of WT (4/5) and Het (13/14) embryos reached and surpassed this threshold, whereas only 1 of 7 *Zc3h4* mutants contained 4 NANOG positive cells (1/7, Figure 3C). In addition to impaired lineage commitment, loss of ZC3H4 also resulted in many DNA breaks and reduced cell proliferation (Figure 4). These results are consistent with a recent study that identified ZC3H4 as an essential factor for cell proliferation in thyroid carcinoma cells [44]. As a novel member in CCCH family, role of ZC3H4 was recently investigated in mouse lung epithelia and cell culture data suggest that ZC3H4 is a pivotal player in epithelial-mesenchymal transition (EMT) during lung fibrosis [43]. Interestingly, as an evolutionarily conserved process, EMT also occurs during embryogenesis and is essential for cell differentiation and lineage specification.

In mammals, the first wave of EMT occurs during implantation that produces trophoblast giant cells from TE that migrate and invade the endometrium [68, 69]. EMT also occurs in the PE to form the parietal endoderm [70]. In order to fully understand the mechanism and specificity of ZC3H4 function during embryogenesis, we will likely need to assess transcriptome wide effects in KO or KD embryos, and possibly perform conditional deletion experiments to determine if there are lineage specific requirements of ZC3H4. Alternatively, ESCs and trophoblast stem cells may serve as good models to explore ZC3H4 function in embryonic pluripotency and trophoblast invasion, respectively.

In summary, using a newly generated *Zc3h4* knockout allele, we demonstrate for the first time that ZC3H4 is essential for early mammalian development in vivo. Loss of ZC3H4 results in defective ICM with consequent reduction of both EPI and PE. Additionally, ZC3H4 KO results in many DNA breaks and reduced cell proliferation, which likely drive the reduced cell numbers and implantation failure resulting in the early lethality of mutant embryos.

Supplementary data

Supplementary data are available at *BIOLRE* online.

Authors' contributions

J. Su and X. Miao contributed equally to this work and performed the majority of the experiments and analyzed the data; D. Archambault performed E5.5 embryo sectioning and immunofluorescence; J. Mager performed E7.5 embryo dissection, initial outgrowth experiments, and characterization of mutant phenotype, helped with experimental design and manuscript preparation; W. Cui contributed to mouse colony maintenance and outgrowth assays, designed the experiments, analyzed the data, and wrote the manuscript. All authors reviewed the manuscript.

Conflict of interest

The authors have declared that no conflict of interest exists.

Acknowledgments

The authors thank the Knockout Mouse Project (KOMP) and Mutant Mouse Resource & Research Centers (MMRRC) for providing *Zc3h4*-knockout allele. We thank Tieqi Sun and Holly Barletta for assistance in genotyping. The confocal microscopy data were gathered in the Light Microscopy Facility and Nikon Center of Excellence at the Institute for Applied Life Sciences, UMass Amherst with support from the Massachusetts Life Sciences Center.

References

1. Arny M, Nachtigall L, Quagliarello J. The effect of preimplantation culture conditions on murine embryo implantation and fetal development. *Fertil Steril* 1987; **48**:861–865.
2. Shi L, Wu J. Epigenetic regulation in mammalian preimplantation embryo development. *Reprod Biol Endocrinol* 2009; **7**:59.
3. Sutherland AE, Calarco-Gillam PG. Analysis of compaction in the preimplantation mouse embryo. *Dev Biol* 1983; **100**:328–338.
4. Houliston E, Maro B. Posttranslational modification of distinct microtubule subpopulations during cell polarization and differentiation in the mouse preimplantation embryo. *J Cell Biol* 1989; **108**:543–551.
5. Latham KE, Solter D, Schultz RM. Activation of a two-cell stage-specific gene following transfer of heterologous nuclei into enucleated mouse embryos. *Mol Reprod Dev* 1991; **30**:182–186.
6. Schall PZ, Ruebel ML, Latham KE. A new role for SMCHD1 in life's master switch and beyond. *Trends Genet* 2019; **35**:948–955.
7. Fleming TP. A quantitative analysis of cell allocation to trophectoderm and inner cell mass in the mouse blastocyst. *Dev Biol* 1987; **119**:520–531.
8. Hogan B, Tilly R. In vitro development of inner cell masses isolated immunosurgically from mouse blastocysts. II. Inner cell masses from 3.5- to 4.0-day p.c. blastocysts. *J Embryol Exp Morphol* 1978; **45**:107–121.
9. Gardner RL. Investigation of cell lineage and differentiation in the extraembryonic endoderm of the mouse embryo. *J Embryol Exp Morphol* 1982; **68**:175–198.
10. Marikawa Y, Alarcon VB. Establishment of trophectoderm and inner cell mass lineages in the mouse embryo. *Mol Reprod Dev* 2009; **76**:1019–1032.
11. Frum T, Ralston A. Cell signaling and transcription factors regulating cell fate during formation of the mouse blastocyst. *Trends Genet* 2015; **31**:402–410.
12. Cui W, Mager J. Transcriptional regulation and genes involved in first lineage specification during preimplantation development. *Adv Anat Embryol Cell Biol* 2018; **229**:31–46.
13. Paul S, Knott JG. Epigenetic control of cell fate in mouse blastocysts: The role of covalent histone modifications and chromatin remodeling. *Mol Reprod Dev* 2014; **81**:171–182.
14. Iqbal K, Chitwood JL, Meyers-Brown GA, Roser JF, Ross PJ. RNA-seq transcriptome profiling of equine inner cell mass and trophectoderm. *Biol Reprod* 2014; **90**:61.
15. Wei Q, Zhong L, Zhang S, Mu H, Xiang J, Yue L, Dai Y, Han J. Bovine lineage specification revealed by single-cell gene expression analysis from zygote to blastocyst. *Biol Reprod* 2017; **97**:5–17.
16. Negron-Perez VM, Zhang Y, Hansen PJ. Single-cell gene expression of the bovine blastocyst. *Reproduction* 2017; **154**:627–644.
17. Niwa H, Toyooka Y, Shimosato D, Strumpf D, Takahashi K, Yagi R, Rossant J. Interaction between Oct3/4 and Cdx2 determines trophectoderm differentiation. *Cell* 2005; **123**:917–929.
18. Strumpf D, Mao CA, Yamanaka Y, Ralston A, Chawengsaksophak K, Beck F, Rossant J. Cdx2 is required for correct cell fate specification and differentiation of trophectoderm in the mouse blastocyst. *Development* 2005; **132**:2093–2102.
19. Yagi R, Kohn MJ, Karavanova I, Kaneko KJ, Vullhorst D, DePamphilis ML, Buonanno A. Transcription factor TEAD4 specifies the trophectoderm lineage at the beginning of mammalian development. *Development* 2007; **134**:3827–3836.
20. Wicklow E, Blij S, Frum T, Hirate Y, Lang RA, Sasaki H, Ralston A. HIPPO pathway members restrict SOX2 to the inner cell mass where it promotes ICM fates in the mouse blastocyst. *PLoS Genet* 2014; **10**:e1004618.
21. Rayon T, Menchero S, Nieto A, Xenopoulos P, Crespo M, Cockburn K, Canon S, Sasaki H, Hadjantonakis AK, de la Pompa JL, Rossant J, Manzanares M. Notch and hippo converge on Cdx2 to specify the trophectoderm lineage in the mouse blastocyst. *Dev Cell* 2014; **30**:410–422.
22. Denicol AC, Block J, Kelley DE, Pohler KG, Dobbs KB, Mortensen CJ, Ortega MS, Hansen PJ. The WNT signaling antagonist Dickkopf-1 directs lineage commitment and promotes survival of the preimplantation embryo. *FASEB J* 2014; **28**:3975–3986.
23. Negron-Perez VM, Rodrigues LT, Mingoti GZ, Hansen PJ. Role of ROCK signaling in formation of the trophectoderm of the bovine preimplantation embryo. *Mol Reprod Dev* 2018; **85**:374–375.
24. Kono K, Tamashiro DA, Alarcon VB. Inhibition of RHO-ROCK signaling enhances ICM and suppresses TE characteristics through activation of hippo signaling in the mouse blastocyst. *Dev Biol* 2014; **394**:142–155.
25. Marcho C, Cui W, Mager J. Epigenetic dynamics during preimplantation development. *Reproduction* 2015; **150**:R109–R120.
26. Chung N, Bogliotti YS, Ding W, Vilarino M, Takahashi K, Chitwood JL, Schultz RM, Ross PJ. Active H3K27me3 demethylation by KDM6B

is required for normal development of bovine preimplantation embryos. *Epigenetics* 2017; **12**:1048–1056.
27. Li Y, Hagen DE, Ji T, Bakhtiarizadeh MR, Frederic WM, Traxler EM, Kalish JM, Rivera RM. Altered microRNA expression profiles in large offspring syndrome and Beckwith-Wiedemann syndrome. *Epigenetics* 2019; **14**:850–876.
28. Chen Z, Hagen DE, Wang J, Elsik CG, Ji T, Siqueira LG, Hansen PJ, Rivera RM. Global assessment of imprinted gene expression in the bovine conceptus by next generation sequencing. *Epigenetics* 2016; **11**:501–516.
29. Cui W, Pizzollo J, Han Z, Marcho C, Zhang K, Mager J. Nop2 is required for mammalian preimplantation development. *Mol Reprod Dev* 2016; **83**:124–131.
30. Wang H, Wang L, Wang Z, Dang Y, Shi Y, Zhao P, Zhang K. The nucleolar protein NOP2 is required for nucleolar maturation and ribosome biogenesis during preimplantation development in mammals. *FASEB J* 2020; **34**:2715–2729.
31. Watanabe Y, Miyasaka KY, Kubo A, Kida YS, Nakagawa O, Hirate Y, Sasaki H, Ogura T. Notch and hippo signaling converge on strawberry notch 1 (Sbno1) to synergistically activate Cdx2 during specification of the trophectoderm. *Sci Rep* 2017; **7**:46135.
32. Cao Z, Carey TS, Ganguly A, Wilson CA, Paul S, Knott JG. Transcription factor AP-2gamma induces early Cdx2 expression and represses HIPPO signaling to specify the trophectoderm lineage. *Development* 2015; **142**:1606–1615.
33. Midic U, Vincent KA, Wang K, Lokken A, Severance AL, Ralston A, Knott JG, Latham KE. Novel key roles for structural maintenance of chromosome flexible domain containing 1 (Smchd1) during preimplantation mouse development. *Mol Reprod Dev* 2018; **85**:635–648.
34. Zhao P, Wang H, Wang H, Dang Y, Luo L, Li S, Shi Y, Wang L, Wang S, Mager J, Zhang K. Essential roles of HDAC1 and 2 in lineage development and genome-wide DNA methylation during mouse preimplantation development. *Epigenetics* 2020; **15**:369–385.
35. Miao X, Sun T, Barletta H, Mager J, Cui W. Loss of RBBP4 results in defective inner cell mass, severe apoptosis, hyperacetylated histones and preimplantation lethality in micedagger. *Biol Reprod* 2020; **103**: 13–23.
36. Ramos SB, Stumpo DJ, Kennington EA, Phillips RS, Bock CB, Ribeiro-Neto F, Blackshear PJ. The CCCH tandem zinc-finger protein Zfp36l2 is crucial for female fertility and early embryonic development. *Development* 2004; **131**:4883–4893.
37. Liang J, Song W, Tromp G, Kolattukudy PE, Fu M. Genome-wide survey and expression profiling of CCCH-zinc finger family reveals a functional module in macrophage activation. *PLoS One* 2008; **3**:e2880.
38. Maeda K, Akira S. Regulation of mRNA stability by CCCH-type zinc-finger proteins in immune cells. *Int Immunol* 2017; **29**:149–155.
39. Rha J, Jones SK, Fidler J, Banerjee A, Leung SW, Morris KJ, Wong JC, Inglis GAS, Shapiro L, Deng Q, Cutler AA, Hanif AM, et al. The RNA-binding protein, ZC3H14, is required for proper poly(a) tail length control, expression of synaptic proteins, and brain function in mice. *Hum Mol Genet* 2017; **26**:3663–3681.
40. Morris KJ, Corbett AH. The polyadenosine RNA-binding protein ZC3H14 interacts with the THO complex and coordinately regulates the processing of neuronal transcripts. *Nucleic Acids Res* 2018; **46**:6561–6575.
41. Pak C, Garshasbi M, Kahrizi K, Gross C, Apponi LH, Noto JJ, Kelly SM, Leung SW, Tzschach A, Behjati F, Abedini SS, Mohseni M, et al. Mutation of the conserved polyadenosine RNA binding protein, ZC3H14/dNab2, impairs neural function in drosophila and humans. *Proc Natl Acad Sci U S A* 2011; **108**:12390–12395.
42. Zou Q, Gang K, Yang Q, Liu X, Tang X, Lu H, He J, Luo L. The CCCH-type zinc finger transcription factor Zc3h8 represses NF-kappaB-mediated inflammation in digestive organs in zebrafish. *J Biol Chem* 2018; **293**:11971–11983.
43. Jiang R, Zhou Z, Liao Y, Yang F, Cheng Y, Huang J, Wang J, Chen H, Zhu T, Chao J. The emerging roles of a novel CCCH-type zinc finger protein, ZC3H4, in silica-induced epithelial to mesenchymal transition. *Toxicol Lett* 2019; **307**:26–40.
44. Geng M, Yang Y, Cao X, Dang L, Zhang T, Zhang L. Targeting CDK12-mediated transcription regulation in anaplastic thyroid carcinoma. *Biochem Biophys Res Commun* 2019; **520**:544–550.
45. Cui W, Dai X, Marcho C, Han Z, Zhang K, Tremblay KD, Mager J. Towards functional annotation of the Preimplantation Transcriptome: An RNAi screen in mammalian embryos. *Sci Rep* 2016; **6**:37396.
46. Cui W, Marcho C, Wang Y, Degani R, Golan M, Tremblay KD, Rivera-Perez JA, Mager J. MED20 is essential for early embryogenesis and regulates NANOG expression. *Reproduction* 2019; **157**:215–222.
47. Cui W, Cheong A, Wang Y, Tsuchida Y, Liu Y, Tremblay KD, Mager J. MCRS1 is essential for epiblast development during early mouse embryogenesis. *Reproduction* 2020; **159**:1–13.
48. Cui W, Zhang J, Zhang CX, Jiao GZ, Zhang M, Wang TY, Luo MJ, Tan JH. Control of spontaneous activation of rat oocytes by regulating plasma membrane Na+/Ca2+ exchanger activities. *Biol Reprod* 2013; **88**:160.
49. Dickinson ME, Flenniken AM, Ji X, Teboul L, Wong MD, White JK, Meehan TF, Weninger WJ, Westerberg H, Adissu H, Baker CN, Bower L, et al. High-throughput discovery of novel developmental phenotypes. *Nature* 2016; **537**:508–514.
50. Zhang Y, Qu P, Ma X, Qiao F, Ma Y, Qing S, Zhang Y, Wang Y, Cui W. Tauroursodeoxycholic acid (TUDCA) alleviates endoplasmic reticulum stress of nuclear donor cells under serum starvation. *PLoS One* 2018; **13**:e0196785.
51. Xue Z, Huang K, Cai C, Cai L, Jiang CY, Feng Y, Liu Z, Zeng Q, Cheng L, Sun YE, Liu JY, Horvath S, et al. Genetic programs in human and mouse early embryos revealed by single-cell RNA sequencing. *Nature* 2013; **500**:593–597.
52. Yi D, Dempersmier JM, Nguyen HP, Viscarra JA, Dinh J, Tabuchi C, Wang Y, Sul HS. Zc3h10 acts as a transcription factor and is phosphorylated to activate the thermogenic program. *Cell Rep* 2019; **29**:2621–2633 e2624.
53. Tanaka Y, Patestos NP, Maekawa T, Ishii S. B-myb is required for inner cell mass formation at an early stage of development. *J Biol Chem* 1999; **274**:28067–28070.
54. Luo S, Mao C, Lee B, Lee AS. GRP78/BiP is required for cell proliferation and protecting the inner cell mass from apoptosis during early mouse embryonic development. *Mol Cell Biol* 2006; **26**:5688–5697.
55. Stephens LE, Sutherland AE, Klimanskaya IV, Andrieux A, Meneses J, Pedersen RA, Damsky CH. Deletion of beta 1 integrins in mice results in inner cell mass failure and peri-implantation lethality. *Genes Dev* 1995; **9**:1883–1895.
56. Dey SK, Lim H, Das SK, Reese J, Paria BC, Daikoku T, Wang H. Molecular cues to implantation. *Endocr Rev* 2004; **25**:341–373.
57. Wu G, Scholer HR. Role of Oct4 in the early embryo development. *Cell Regen (Lond)* 2014; **3**:7.
58. Daigneault BW, Rajput S, Smith GW, Ross PJ. Embryonic POU5F1 is required for expanded bovine blastocyst formation. *Sci Rep* 2018; **8**: 7753.
59. Rodda DJ, Chew JL, Lim LH, Loh YH, Wang B, Ng HH, Robson P. Transcriptional regulation of nanog by OCT4 and SOX2. *J Biol Chem* 2005; **280**:24731–24737.
60. Simmet K, Zakhartchenko V, Philippou-Massier J, Blum H, Klymiuk N, Wolf E. OCT4/POU5F1 is required for NANOG expression in bovine blastocysts. *Proc Natl Acad Sci U S A* 2018; **115**:2770–2775.
61. Le Bin GC, Munoz-Descalzo S, Kurowski A, Leitch H, Lou X, Mansfield W, Etienne-Dumeau C, Grabole N, Mulas C, Niwa H, Hadjantonakis AK, Nichols J. Oct4 is required for lineage priming in the developing inner cell mass of the mouse blastocyst. *Development* 2014; **141**: 1001–1010.
62. Ueno M, Itoh M, Kong L, Sugihara K, Asano M, Takakura N. PSF1 is essential for early embryogenesis in mice. *Mol Cell Biol* 2005; **25**:10528–10532.
63. Fang L, Zhang J, Zhang H, Yang X, Jin X, Zhang L, Skalnik DG, Jin Y, Zhang Y, Huang X, Li J, Wong J. H3K4 Methyltransferase Set1a is a key Oct4 Coactivator essential for generation of Oct4 positive inner cell mass. *Stem Cells* 2016; **34**:565–580.
64. Li L, Walsh RM, Wagh V, James MF, Beauchamp RL, Chang YS, Gusella JF, Hochedlinger K, Ramesh V. Mediator subunit Med28 is essential for

mouse peri-implantation development and pluripotency. *PLoS One* 2015; **10**:e0140192.

65. Nichols J, Zevnik B, Anastassiadis K, Niwa H, Klewe-Nebenius D, Chambers I, Scholer H, Smith A. Formation of pluripotent stem cells in the mammalian embryo depends on the POU transcription factor Oct4. *Cell* 1998; **95**:379–391.
66. Wen J, Lv R, Ma H, Shen H, He C, Wang J, Jiao F, Liu H, Yang P, Tan L, Lan F, Shi YG, et al. Zc3h13 regulates nuclear RNA m(6)A methylation and mouse embryonic stem cell self-renewal. *Mol Cell* 2018; **69**:1028, e1026–1038.
67. Morris SA, Guo Y, Zernicka-Goetz M. Developmental plasticity is bound by pluripotency and the Fgf and Wnt signaling pathways. *Cell Rep* 2012; **2**:756–765.
68. Abell AN, Granger DA, Johnson NL, Vincent-Jordan N, Dibble CF, Johnson GL. Trophoblast stem cell maintenance by fibroblast growth factor 4 requires MEKK4 activation of Jun N-terminal kinase. *Mol Cell Biol* 2009; **29**:2748–2761.
69. Chakraborty D, Cui W, Rosario GX, Scott RL, Dhakal P, Renaud SJ, Tachibana M, Rumi MA, Mason CW, Krieg AJ, Soares MJ. HIF-KDM3A-MMP12 regulatory circuit ensures trophoblast plasticity and placental adaptations to hypoxia. *Proc Natl Acad Sci U S A* 2016; **113**:E7212–E7221.
70. Veltmaat JM, Orelio CC, Ward-Van Oostwaard D, Van Rooijen MA, Mummery CL, Defize LH. Snail is an immediate early target gene of parathyroid hormone related peptide signaling in parietal endoderm formation. *Int J Dev Biol* 2000; **44**:297–307.